First published in:

V-IV-03

IWPMA 2005
2nd International Workshop on Piezoelectric Materials and Applications in Actuators

Studies On Nonlinear Electromechanical Behavior Of Piezoelectric Materials Using Finite Element Modeling

A. Arockiarajan[1], B. Delibas[1], A. Menzel[1], W. Seemann[2]

[1] Chair of Applied Mechanics, University of Kaiserslautern, Kaiserslautern, GERMANY

[2] Institute for Engineering Mechanics, University of Karlsruhe, Karlsruhe, GERMANY

Abstract: The main goal of this paper consists in the modeling of nonlinear behavior of piezoelectric materials within a non linear finite element setting. The model accounts for differently oriented grains. Uni-axial, quasi-static loading is applied in the simulations. The reduction in free energy of a grain is used as a criterion for the domain switching process. Averaging over all individual grains renders the macroscopic response of the bulk material. Intergranular effects, which are essential for realistic simulations, are phenomenologically captured via a probabilistic approach. In particular, averaged electric displacement versus electric field curves and electric displacement versus strain are plotted and compared with experimental data reported in the literature.

Keywords: Finite element method, Non linear behavior, Probabilistic approach.

1. Introduction

In recent years, piezoelectric and ferroelectric materials served as smart materials and have already been applied in various areas, for example, vibration damping and noise control, precision positioning and cutting, injection mechanism in common rail systems with piezo control in automobiles, smart aircrafts, smart system for bridges and highways. Even though these materials are widely used in many applications they still have some restrictions. These materials exhibit nonlinear behavior when they are subjected to high electromechanical loading. The dominating nonlinearity in piezoelectric materials is the result of domain switching which is the change of the direction of the spontaneous polarization in the microstructure under high electromechanical loadings. Modeling of nonlinear response of piezoceramics can be distinguished into two major approaches: the first approach is focused on micromechanical modeling. Each domain is commonly assumed as one element which is randomly oriented. The macroscopic behavior of the bulk ceramics are analysed by means of volume averaging. A micromechanical model of ferroelectric, ferroelastic polycrystals using finite element were developed by Hwang [1-2]. It is assumed that a crystallite switches if the reduction in potential energy of the polycrystal exceeds a critical energy barrier per unit volume of switching material. The contribution of combined electrical and mechanical

loading to switching in ferroelectric/ferroelastic polycrystals was studied by the same author [3] by using a similar approach while piezoelectric effect was neglected to reduce the computational effort. Another approach [4] was developed by addressing the domain switching criterion based on a critical value of the electric displacement due to switching with additional stability arguments for mono-crystalline piezoceramics. The second approach focuses on phenomenological (macroscopic) models which are usually based on a thermodynamically consistent framework and are developed to predict the behavior of ferroelectric materials. A basic phenomenological model [5-6] for ferroelectric materials is elaborated with certain internal variables that are introduced in the model. The constitutive behavior is governed by appropriate ordinary differential equations capturing the history dependence of the material. In this work, polarization switching in piezoelectric materials is simulated using finite element model by micromechanical approach. The model accounts for differently oriented grains. The response of the macroscopic behavior of bulk ceramics is predicted by averaging the response of individual grains. It is assumed that a domain switches if the reduction in free energy of the polycrystal exceeds a threshold of critical energy per unit volume of the material. In general, domain switching may occur below the critical energy level due to intergranular effects. This effect is modeled by introducing a polynomial probability function for domain switching related to actual energy level to the critical energy level. Using the domain switching and probability function, the behavior is simulated without any superimposed stress, and then with the influence of a superimposed compression.

2. Constitutive model

Assume that a piezoelectric material occupies a volume (V) added with a closed surface (S). The mechanical equilibrium equation can be written as (without considering the body force):

$$\partial \tau_{ij} / \partial x_i = 0_j \tag{1}$$

The continuity of stress, at the boundaries:

$$n_i \left[\left| \tau_{ij} \right|\right] = 0_j \tag{2}$$

The conservation of charge:

$$\partial D_i / \partial x_i = 0 \tag{3}$$

The continuity of charge, at the boundaries:

$$n_i \left[\left| D_i \right|\right] = 0 \tag{4}$$

The strain can be expressed by the mechanical displacement:

$$e_{ij} = (u_{i,j} + u_{j,i}) / 2 \tag{5}$$

The electric field can be expressed by the negative potential of electric potential

$$E_i = -\partial \phi / \partial x_i \tag{6}$$

The linear response of piezoelectric materials are given by the constitutive equations

$$\tau_{ij} = C_{ijkl} e_{kl} - d_{kij} E_k \tag{7}$$

$$D_i = d_{ikl} e_{kl} + \varepsilon_{ij} E_j \tag{8}$$

where u_i is the displacement vector, e_{ij} the strain tensor, τ_{ij} the stress tentor, ϕ the electric potential, D_i the electric displacement vector, E_i the electric field vector, C_{ijkl} the elastic constitutive tensor, d_{kij} the piezoelectric tensor, ε_{ij} the dielectric permittivity tensor, n the unit normal to the surface and x_i the position vector.

Nonlinear constitutive equations of the piezoelectric material additionally incorporate a spontaneous polarization vector and a spontaneous strain tensor. The extension of eqs. (7, 8) consequently renders

$$\tau_{ij} = C_{ijkl}(e_{kl} - e^s_{kl}) - d_{kij}E_k \tag{9}$$

$$D_i = d_{ikl}(e_{kl} - e^s_{kl}) + \varepsilon_{ij}E_j + P^s_i \tag{10}$$

where e_{kl}^s the spontaneous strain and P_i^s the spontaneous polarization. During the domain switching, most of the material constants will change in general. In this work, however, the dielectric constant and elastic constant are kept constant and represent isotropic response. However the piezoelectric constants usually change significantly during switching. To take into account of this phenomenon, these constants are proportional to the remnant polarization [5].

$$\varepsilon_{ij} = \varepsilon\delta_{ij} \tag{11}$$

$$C_{ijkl} = \frac{Y\upsilon}{(1+\upsilon)(1-2\upsilon)}\delta_{ij}\delta_{kl} - \frac{Y}{2(1+\upsilon)}(\delta_{ik}\delta_{jl} + \delta_{il}\delta_{jk}) \tag{12}$$

$$\bar{d}_{kij} = \frac{\overline{P^s}}{P_0}\cdot d_{kij} \tag{13}$$

where Y the Young's modulus, υ the poisson's ratio, $\overline{P^s}$ the current average spontaneous polaration value and P_0 the critical spontaneous polarization value. The main reason for nonlinear behavior of the material stems from domain switching effects in the microstructure. There are six possible orientations for the polarization in the lattice structure for a perovskite type tetragonal microstructure. Therefore, only two types of domain switching are possible. 90° and 180° domain switching are related to the angle of rotation of the polarization vector. A crystallite microstructure is commonly considered to switch, if the reduction of free energy exceeds a particular energy barrier. In this work we adopt the switching criterion, along with boundary conditions, by McMeeking [7]

$$\Delta U(u_i, \phi) + V_c\Delta\psi_c \le 0 \tag{14}$$

Where $\Delta\psi_c$ denotes a constant energy barrier per unit volume and V_c represents the volume of the crystallite which switches. The change of energy in the system is approximated [8] and incorporated into the switching criterion in eq. (14) which enables us to compute representative numerical examples in this work.

$$\Delta U = E_i \Delta P_i^s + \tau_{ij} \Delta e_{ij}^s \tag{15}$$

Apparently, the constitutive framework reviewed so far fits into the class of coupled problems. The degrees of freedom, namely u_i and ϕ, are coupled and the constitutive equations eqs. (9, 10). It is obvious that any change in spontaneous polarization or spontaneous strain consequently contributes to the iterative calculation of the displacement field and the electric potential, respectively.

3. Finite Element Formulation

In this section we review the algorithmic setting which will enable us to run numerical simulations. In particular, the finite element method is used and applied within a two-dimensional context. Based on piezoelectric constitutive laws and balance equations, the finite element formulation are derived from the principle of virtual work. By considering the experimental setup, the (essential) boundary conditions might be covered by electrodes - prescribing the electric potential - while the (natural) boundary conditions represent a prescribed charge for the electrical case.

$$n_i D_i = -q \quad \text{on } S_q \tag{16}$$

$$\phi = \phi^0 \quad \text{on } S_\phi \tag{17}$$

Similarly the (essential) boundary conditions are prescribed the displacements while the (natural) boundary conditions are represented by prescribed tractions for the mechanical case.

$$n_i \tau_{ij} = t_j \quad \text{on } S_t \tag{18}$$

$$u_i = u_i^0 \quad \text{on } S_u \tag{19}$$

With these definitions at hand, the corresponding weak form results in

$$\int_V \left[\tau_{ij} \delta u_{i,j} + D_i \delta \phi_i\right] dV - \int_{S_t} (\tau_{ij} n_j - t_i) \delta u_i dS - \int_{S_q} (D_i n_i - q) \delta \phi dS = 0 \tag{20}$$

The approximated displacement and electric potential can be expressed in the matrix notation as:

$$\begin{Bmatrix} U_x \\ U_y \end{Bmatrix} = [N_u]\{u_N\} \tag{21}$$

$$\phi = [N_\phi]\{\phi_N\} \tag{22}$$

where N_u and N_ϕ represent the interpolation function for displacements and the electric potential. In the same way, the strain and electric field can be expressed as

$$\{e_{xx}\ e_{yy}\ 2e_{xy}\} = \{e\} = [B_u]\{u_N\} \tag{23}$$

$$\{E_x\ E_y\} = \{E\} = [B_\phi]\{\phi_N\} \tag{24}$$

Use of the modified constitutive laws equations (9) and (10) gives the incremental finite element equation

$$[K]\{\Delta u\} = \{F\} + \{F^s\} \tag{25}$$

$$\text{where } [K] = \begin{bmatrix} K_u & K_{u\phi} \\ K_{\phi u} & K_\phi \end{bmatrix}, \quad \{\Delta u\} = \begin{Bmatrix} \Delta u_N \\ \Delta \phi_N \end{Bmatrix}, \quad \{F\} = \begin{Bmatrix} F_u \\ F_\phi \end{Bmatrix}, \quad \{F^s\} = \begin{Bmatrix} F_u^s \\ F_\phi^s \end{Bmatrix} \tag{26}$$

$$[K_u] = \int_V [B_e]^T [C][B_e]\, \mathrm{d}V, \qquad [K_{u\phi}] = -\int_V [B_e]^T [d][B_E]\, \mathrm{d}V, \tag{27}$$

$$[K_{\phi u}] = -\int_V [B_E]^T [d]^T [B_e]\, \mathrm{d}V, \qquad [K_\phi] = -\int_V [B_E]^T [\varepsilon][B_E]\, \mathrm{d}V$$

$$\{F_u\} = \int_{S_t} [N_u]^T \{t\}\, \mathrm{d}S, \qquad \{F_\phi\} = \int_{S_q} [N_\phi]^T q\, \mathrm{d}S$$

$$\{F_u^s\} = \int_V [B_e]^T [C]\{e^s\}\, \mathrm{d}V, \qquad \{F_\phi^s\} = \int_V [B_E]^T \{P^s\}\, \mathrm{d}V$$

3. Numerical Examples

The computation of the material behavior is performed within a two-dimensional finite element scheme, whereby four-node elements based on standard linear (Legendre) shape functions are adopted. Some hundreds of crystallites are modeled so that each finite element represents one crystallite; see the graphical representation in Fig.1. Moreover, we assume the polarization vector to be constant within each element, or rather crystallite, and choose a random orientation for the initial polarization vector. The traction and electric potential are imposed on the top edge of the square. At the bottom edge the displacement is fixed and the electric potential is zero. A uniform electric potential is applied incrementally at the nodal points on the top edge and constant traction is applied at the nodal points on the top edge. After a small load increment with electric potential, each crystallite is checked to see if it has met the switching criterion in

$$E_i \Delta P_i^s + \sigma_{ij} \Delta e_{ij}^s \geq 2E_0 P_0 \tag{28}$$

Where ΔP_i^s, Δe_{ij}^s represents the switched state of spontaneous polarization and strain. E_0, P_0 are the critical electric field and spontaneous polarization. According to this criterion, domain switching occurs if the energy change is higher than a certain critical level for one element at a time. In this simulation, the critical energy barrier is assumed to be identical for 90^0 and

180^0 switching. If switching occurs according to the mentioned criteria, new nodal loads $\{F_u^s\}$ and $\{F_\phi^s\}$ in equation (25) are computed by reassembling the spontaneous polarization of the crystallites in the finite element. Solving for equation (25) with the new $\{F^s\}$ gives the new electric potential, electric field, displacement and stress in each element. Due to the computational limitation, we compute all possible domain switchings for the grains and allow the maximum possibility domain to switch.

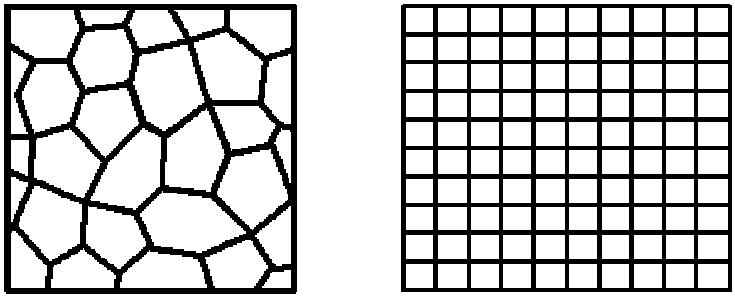

Fig.1 Natural assembly of grains and finite element discretization

The orientations of spontaneous polarization of all grains in one domain of interest are different from the orientations in other domains for piezoelectric materials. The electromechanical loading values might considerably vary between grains, so that domain switching can occur for some lattice structures even below the assumed critical electromechanical field. As a result, nonlinear response is observed even in a small electromechanical loading range. In order to take this effect into account, which becomes especially relevant in the domain switching range, the proposed formulation incorporates an additional probability function for the domain switching. In what follows, we assume this function to be determined via the polynomial

$$P(E_i) = \left(\|E_i\| \,/\, E_0\right)^n \quad \text{for} \quad \|E_i\| \le E_0 \qquad (29)$$
$$P(E_i) = 1 \quad \text{for} \quad \|E_i\| \ge E_0$$

The value of the probability (P) is varying between 0 and 1 according to the applied electric field. When the applied electric field is higher than or equal to the critical electric field, the probability value is taken as 1. In the described model n is an unknown parameter the value of which can be chosen arbitrarily in order to get optimum matching of the results to experimental data. In this simulation, n is chosen as four and five. All calculations in this paper are done with an identical set of around 700 elements with random polarization. The elements are arranged in a 26 x 26 array of equal sized 2-D isoparametric elements whereby the edges are parallel to a global cartesian coordinate system. The electric field, electric displacement, stress and strains are evaluated at each Gauss point in the element. During the calculation, the value for Young's modulus (Y), Poisson's ratio (υ) and dielectric constant (ε) are taken as 30 GPa, 0.3 and 0.0666 μF/m. The other parameters are: the piezoelectric constant (d_{333}) = 1.52 x

10^{-9} m/V, (d_{311}) = -0.57 x 10^{-9} m/V, (d_{113}) = 1.856 x 10^{-9} m/V the critical polarization (P_0) = 0.1938 C/m^2, the critical electric field (E_0) = 0.4 MV/m which are chosen to provide good agreement of the model with the experimental data. Volume averaging of all grains is used to get the macroscopic response of the bulk material to the electromechanical loading. Fig. 2 – 4 show only electrical loading without any mechanical stress is applied. A cyclic and uni-axial electric potential is applied for the simulations. The starting point for the first cycle is at zero potential for the unpoled ceramic. Fig. 2(a) shows an electric displacement versus electric field hysteresis curve without considering a probability function in the simulation for quasi-static loading. In this figure, the hysteresis curve has a sharp corner near the critical electric field, which is the main difference of the model compared to experimental data.

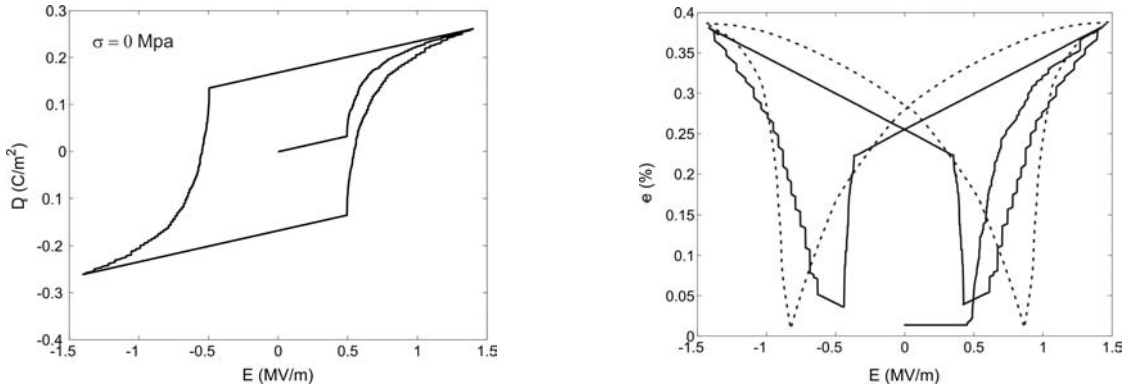

Fig.2 (a, b) Hysteresis and Butterfly curve –Without probability

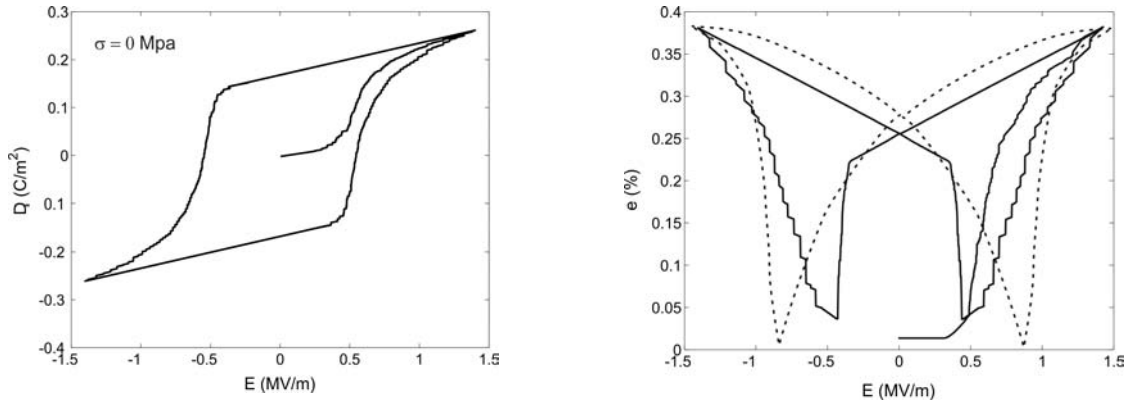

Fig.3 (a, b) Hysteresis and Butterfly curve – Fourth order probability function

Fig. 3(a) shows the curve in which a fourth order polynomial for the probability function is implemented. Smoothness of the curves near the critical electric field can be easily observed. Subsequently, a fifth orfer polynomial is also implemented and shown in Fig. 4(a). The simulated results obtained with a fifth order probability function fit better to experimental results than those curves[9], which were simulated without using probability criteria. Fig. 2(b)

shows an electric displacement vesus longitudinal stain curve without considering a probability function. The sharp corners are also predicted similar to the hysteresis curve. Fig . 3(b) & 4(b) shows the butterfly curves implemented with fourth and fifth order probability functions. The simulated results obtained with a fifth order probability function fit better to experimental results than those curves, which were simulated without using probability criteria.

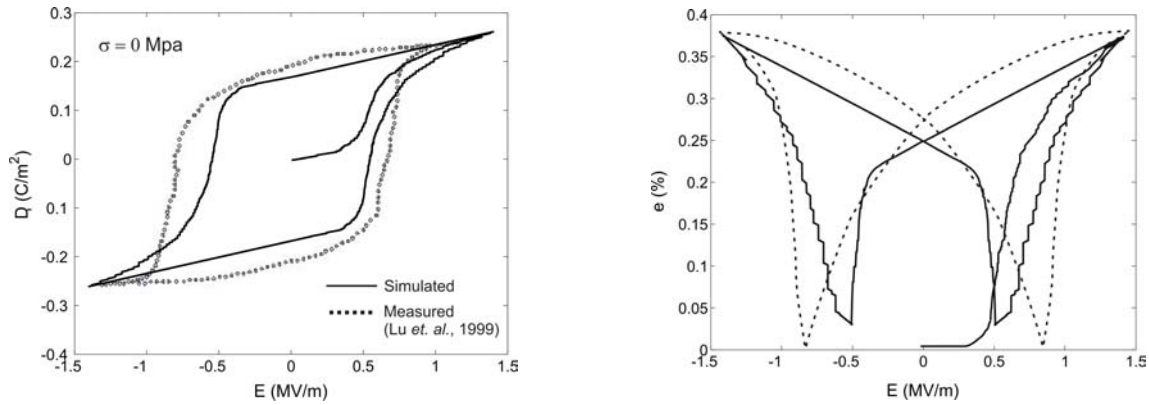

Fig.4 (a, b) Hysteresis and Butterfly curve – Fifth order probability function

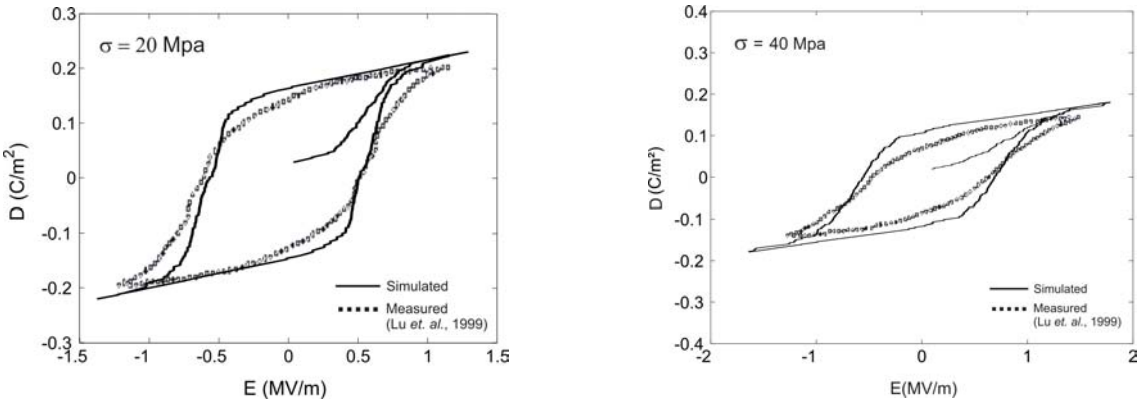

Fig.5 (a, b) Hysteresis curves – Fifth order probability function

Fig. 5 shows results of a computation where cyclic uni-axial electric potential and a constant compressive stress are applied according to the loading direction. In the electromechanical loading, some differences are observed in the hysteresis curve compared with electrical loading. A decreasing of the coercive electric field value which is the threshold for domain switching is the first observation. This is because of the domain switching under the loading of compressive stress. It is experimentally proven that there occur more 90° domain switchings under mechanical loading than without mechanical loading [9]. The basic reason for decreasing of the critical electric field level is the reduction of free energy required for domain switching for the first 90° domain switching due to the stress distribution inside the microstructure of the material. Another observation of the constant compressive stress is the

reduction of remnant and saturation polarization values of the hysteresis curves. This can be explained by the linear constitutive equation. Due to electromechanical loading, the piezoelectric constant also changes nonlinearly. Figs. 5a and b show the hysteresis curves at 20 Mpa and 40 Mpa constant compressive stress and compare these results with experimental data. As the constant compressive stress is increased, the range of domain switching is enlarged which is approximated well in the simulation. However, the magnitude of change of macroscopic electric displacement has been overestimated.

4. Conclusion

A micromechanical model based on a non linear finite element approach is proposed in this paper in order to simulate and analyze the nonlinear behavior of piezoelectric ceramics. The simulations are performed with uni-axial, quasi-static, high cyclic electric loading and constant compressive stress. The model is not only based on a linear constitutive model but also on nonlinear domain switching added with probability functions. The simulated hysteresis and butterfly curves, using probability functions have good agreement with experimental hysteresis curves. Piezoelectric materials subjected to various constant compressive stress have been addressed in this paper. In future work, the focus will be concentrated on micromechanically deriving intergranular effects between neighboring grains.

5. Acknowledgements

The authors thank the 'Deutsche Forschungsgemeinschaft (DFG) for financial support of this work within the Graduiertenkolleg 814, Ingenieurmaterialien auf verschiedenen Skalen: Experiment, Modellierung und Simulation.

References

[1] S.C. Hwang., and R.M. McMeeking., A finite element model of ferroelectric polycrystals, *Ferroelectrics*, 211(1997), 177-194.

[2] S.C. Hwang., and R.M. McMeeking., A finite element model of ferroelastic polycrystals, *Int. Journal of Solids and Structures*, 36(1999), 1540-1556.

[3] S.C. Hwang., and R. Waser., Study of electrical and mechanical contribution to switching in ferroelectric and ferroelastic polycrystals, *Acta Mater*, 48(2000), 3271-3282.

[4] Y. Fotinich., and G.P. Carman., Stresses in piezoceramics undergoing polarization switchings, *Journal of Applied Physics*, 88(2000), 6715-6725.

[5] M. Kamlah., and C. Tsakmakis., Phenomenological modeling of non-linear electromechanical coupling in ferroelectrics, *Int. Journal of Solids and Structures*, 36(1999), 666-678.

[6] M. Kamlah., and U. Böhle., Finite element analysis of piezoceramic components taking into account ferroelectric hysteresis behavior in ferroelectrics, *Int. Journal of Solids and Structures*, 388(2001), 605-633.

[7] R. M. McMeeking., and S.C. Hwang, On the potential energy of a piezoelectric inclusion and the criterion for ferroelectric switching, *Ferroelectrics*, 200(1997), 151-173.

[8] S.C Hwang, C.S. Lynch, and R.M. McMeeking, Ferroelectric/ferroelastic interactions and a polarization switching model. *Acta Metallurgica of Materialia*, 5(1995), 2073-2084.

[9] W. Lu., D. N. Fang., C.Q. Li., and K.C.Hwang, Nonlinear electric-mechanical behavior and micromechanics modeling of ferroelectric domain evolution, *Acta Mater.*, 47(1999), 2913-2926.